1  The relative importance of antecedent soil moisture and precipitation

2      in flood generation in the middle and lower Yangtze River basin

4  Sheng Ye[1], Jin Wang[1], Qihua Ran[2]*, Xiuxiu Chen[1], Lin Liu[1]

6  [1] Institute of Hydrology and Water Resources, School of Civil Engineering, Zhejiang

7  University, Hangzhou 310058, China

8  [2] State Key Laboratory of Hydrology-Water Resources and Hydraulic Engineering,
9  Hohai University, Nanjing 210098, China

11  * Corresponding author: Qihua Ran

13  Email address of the corresponding author: ranqihua@zju.edu.cn

15  April 21, 2022

19  **Abstract**

20  Floods have caused severe environmental and social economic losses worldwide in

21  human history, and are projected to exacerbate due to climate change. Many floods are

22  caused by heavy rainfall with highly saturated soil, however, the relative importance of

23  rainfall and antecedent soil moisture and how it changes from place to place has not

24  been fully understood. Here we examined annual floods from more than 200

25  hydrological stations in the middle and lower Yangtze River basin. Our results indicate

26  that the dominant factor of flood generation shifts from rainfall to antecedent soil

27  moisture with the increase of watershed area. The ratio of the relative importance of

28  antecedent soil moisture and daily rainfall (SPR) is positively correlated with

29  topographic wetness index and has a negative correlation with the magnitude of annual

30  floods. This linkage between watershed characteristics that are easy to measure and the

31  dominant flood generation mechanism provides a framework to quantitatively estimate

32  potential flood risk in ungauged watersheds in the middle and lower Yangtze River

33  basin.

34  **Key words**: flood generation, scaling effect, topographic wetness index

## 1. Introduction

Flooding is one of the most destructive and costly natural hazards in the world, resulting in considerable fatalities and property losses (Suresh et al., 2013). River floods have affected nearly 2.5 billion people between 1994 and 2013 worldwide (CRED, 2015), and caused 104 billion dollars losses every year (Desai et al 2015). The damages may be further exacerbated by increasing frequency and intensity of extreme rainfall events according to climate change projection (IPCC 2012; Ohmura and Wild 2002). Flood control infrastructures and more accurate predictions are needed to reduce flood damages, which requires better understanding of the underlying mechanism of flood generation as well as the drivers of change (Villarini & Wasko 2021).

Numerous studies have been conducted to investigate the cause of floods across the world (Bloschl et al 2013; Munoz et al 2018; Zhang et al 2018). Many studies focused on examining the environmental and social characteristics that lead to specific catastrophic flood events (Bloschl et al 2013; Liu et al 2020; Zhang et al., 2018). Others concentrated on single locations, usually catchment outlets, to explore the influential factors of floods and the future trends (Brunner et al., 2016; Munoz et al 2018). Yet given the amount of data and time required, it is not practical to apply these detailed studies to hundreds of catchments to generate an overview of the flood generation mechanism at large scale.

Recently, researchers started to investigate the dominant flood generation mechanisms at regional scales (Berghuijs et al 2019b; Do et al 2020; Garg & Mishra 2019; Smith et al 2018; Tramblay et al 2021; Ye et al 2017). Most of these studies are conducted in North America and Europe with well-documented long-term records (Berghuijs et al 2016; Bloschl et al 2019; Do et al 2020; Musselman et al 2018; Rottler

61    et al 2020). Such researches were just conducted in China recently, though still limited

62    (Yang et al 2019; Yang et al 2020).

63        As the largest river in China, Yangtze River basin has long suffered from floods. In

64    summer 2020, 378 tributaries of the Yangtze River had floods exceeding the alarm level,

65    causing billions of dollars damage (Xia et al., 2021). With the increasing public

66    awareness, more accurate prediction is needed, which relies on better understanding.

67    However, due to the limitation of observations, there are only a few regional studies of

68    the flood generation mechanism in China, even little in the Yangtze River basin (Zhang

69    et al 2018; Yang et al 2019; Yang et al 2020). The large number of dams and reservoirs

70    built along the river further complicated the situation (Feng et al., 2017; Qian et al 2011;

71    Yang et al 2019).

72        Because of the relatively warm temperature, snowmelt has little impact on flood

73    generation in the Yangtze River basin (Yang et al 2020). Floods in the Yangtze River

74    basin usually occur during summer with relatively wet soil and high rainfall (Wang et

75    al 2021). Heavy rainfall with high antecedent soil moisture has also been identified as

76    dominant driver of floods across world (Beighuijs et al 2019b; Garg et al 2019;

77    Tramblay et al 2021; Wasko et al 2020). Recently, studies started to examines the

78    relative importance of rainfall and antecedent soil moisture in flood generation

79    (Brunner et al., 2021; Wasko et al., 2021; Bennett et al., 2018; Bertola et al., 2021).

80    Quantitative evaluation of the relative contribution of rainfall and antecedent soil

81    moisture and its change across watersheds is still limited and currently unavailable in

82    China (Liu et al., 2021; Wu et al., 2015).

83        Based on the watersheds in the middle and lower Yangtze River basin, this study

84    attempts to explore the following questions: 1) is there a way to quantitatively describe

85  the relative importance of antecedent soil moisture and rainfall on flood generation; and

86  2) how would this combination of flood-generation rainfall and soil moisture vary

87  across watersheds, and what are the influential factors. Based on the observations and

88  model estimation (Section 2), the spatial distribution patterns of antecedent soil

89  moisture and rainfall were obtained and analyzed to investigate their individual

90  contribution to flood generation and the influential factors (Section3). This allows for

91  further examination of the relative importance of antecedent soil moisture and rainfall

92  on flood generation and its linkage to watershed characteristics as well as its

93  implications to flood prediction (Section 4), all the results are summarized in Section 5.

94  **2 Methods**

95  **2.1 Study area**

96  The Yangtze River is the largest river in China, with a total length of 6,300 kilometers

97  and annual discharge of 920km$^3$ at the outlet (Yang et al., 2018). It drains through an

98  area of 1.8*10$^6$ km$^2$, lying between 90°33'and 122°25'E and 24°30'and 35°45'N, and

99  is home to over 400 million people, most of which live in the middle and lower Yangtze

100 River basin (YZRB) (Cai et al., 2020). The elevation of the YZRB declines from west

101 to east: from over 3000m in Qinghai-Tibet Plateau, to around 1000m in the central

102 mountain region, and the 100m in Eastern China Plain (Wang et al., 2013). The

103 vegetation types in the YZRB are forests, shrubs, grassland and agricultural land,

104 accounting for 11.85%, 12.65%, 32.26% and 42.88% respectively. Grassland and

105 shrubs are the dominant vegetation in the middle and upper YZRB, while the

106 downstream YZRB is dominated by forests and agricultural land (Miao et al., 2010).

107 There are more than 51,000 reservoirs of different sizes in the whole basin, including

108 280 large ones (Peng et al., 2020).

109    Most of the YZRB is semi-humid and humid, with a typical subtropical monsoon

110    climate. The mean annual temperature is approximately 13.0 °C, varying from −4 °C

111    to 18°C downstream. The mean annual precipitation of the whole basin is about 1200

112    mm, increasing from 300mm in the western headwaters to 2400 mm downstream. (Li

113    et al., 2021). Most of the precipitation comes between June and September, the premise

114    of persistent heavy rain in the Yangtze River basin is the frequent activity of weak cold

115    air in the north (Tao et al., 1980) and the intersection of mid-latitude air mass and

116    monsoon air mass (Kato et al., 1985). Studies have found that both annual precipitation

117    and the frequency of extreme precipitation events have increased in the middle and

118    lower reaches of the Yangtze River (Qian et al., 2020; Fu et al., 2013). As a result, floods

119    have occurred frequently in the middle and lower reaches of the Yangtze River, where

120    most of the population in the YZRB live (Liu et al., 2018).

121    **2.2 Data**

122    In this work, we focus on the middle and lower reaches of the Yangtze River for the

123    high population density and increasing flood risk. The 30-meter digital elevation model

124    (DEM) was downloaded from Geospatial Data Cloud (http://www.gscloud.cn/), from

125    which the drainage area corresponding to the hydrological station was extracted by

126    ArcGIS. Daily precipitation data and temperature data between 1970 and 2016 from

127    247 meteorological stations within and near the YZRB were downloaded from China

128    Meteorological Data Network (https://data.cma.cn/) (Figure 1). The temperature data

129    was used to estimate potential evaporation. The observed precipitation and estimated

130    potential evaporation were interpolated into the whole YZRB using Thiessen polygon

131    method (Meena et al., 2013). The interpolated precipitation and potential evaporation

132    were then averaged for the drainage area corresponding to each hydrological station.

133    The daily streamflow data was collected from 267 hydrological stations from

134    Annual Hydrological Report of the People's Republic of China. Among which, 224

135    stations with at least 20 years records from both the period from 1970 to 1990 and the

136    period from 2007 to 2016 were selected (see Figure S1 for data availability).

137    Information of 361 reservoirs in the middle and lower YZRB, including capacity and

138    controlling area was downloaded and extracted from the Global Reservoir and Dam

139    database (GRanD) (Lehner et al 2011). Previous study showed that this database

140    provides reliable information of middle and large reservoirs in China (Yang et al 2021).

141    Watersheds with more than 80% of the drainage area under control reservoirs according

142    to GRanD database and/or located right downstream of reservoirs and water gates were

143    considered as watersheds under strong regulation (regulated watersheds).

144    **2.3 Calculation of hydrological and topographic characteristics**

145    *Potential evaporation estimation*

146    The temperature data was used to estimate potential evaporation following the

147    Hargreaves method (Allen et al., 1998; Vicente et al., 2014; Berti et al., 2014).

148    $$ET_0 = 0.0023 \times (Tmax - Tmin)^{0.5} \times (Tmean + 17.8) \times Ra \qquad (1)$$

149    where $ET_0$ is potential evaporation (mm/d), $Tmax$ is the highest temperature (°C), $Tmin$

150    is the lowest temperature (°C), $Tmean$ is the mean temperature (°C), and $Ra$ is the outer

151    space radiation [MJ/(m$^2$·d)], which can be calculated as follows:

152    $$Ra = 37.6 \times d_r \times (\omega_s \sin \varphi \sin \delta + \cos \varphi \cos \delta \sin \omega_s), \qquad (2)$$

153    where $d_r$ is the reciprocal of the relative distance between the sun and the earth, $\omega_s$ is

154    the angle of sunshine hours, $\delta$ is the inclination of the sun (rad), $\varphi$ is geographic

latitude (rad). $d_r$, $\delta$ and $\omega_s$ can be calculated by the following formula:

$$d_r = 1 + 0.033 \times \cos\left(\frac{2\pi J}{365}\right),\tag{3}$$

$$\delta = 0.409 \times \sin\left(\frac{2\pi J}{365} - 1.39\right),\tag{4}$$

$$\omega_s = \arccos(-\tan\varphi\tan\delta)\ ,\tag{5}$$

where $J$ is the daily ordinal number (January 1st is 1).

*Soil water storage estimation*

The soil water storage was estimated based on the daily water balance (Berhuijs et al., 2016, 2019):

$$\frac{dS}{dt} = P - ET - \max(Q, 0),\tag{6}$$

Where $S$ is the soil water storage (mm), which is initially set to 0. Due to the long term of simulation, the change of initial value wouldn't significantly affect the results. $P$ is precipitation (mm/d), $Q$ is discharge normalized by area (mm/d), $ET$ is evaporation (mm/d), which can be calculated from potential evapotranspiration ($ET_0$), where the soil water storage ($S$) is used as the upper limit of daily ET:

$$ET = \min(0.75 \times ET_0, S),\tag{7}$$

The estimation of soil water storage and ET are highly simplified and is not used for prediction but to capture the first order of the seasonal variation and to help develop a framework that differentiates the relative contribution of precipitation and soil moisture in flood generation.

174 *Topographic wetness index estimation*

175 Topographic wetness index was calculated to represent the combined impacts of

176 drainage area and topographic gradient (Alfonso et al., 2011; Grabs et al., 2009):

177 $$TWI = \ln(A_d/\tan\alpha),\qquad(8)$$

178 where $A_d$ is drainage area and $\alpha$ is topographic gradient estimated from DEM. TWI

179 represents the propensity of subsurface flow accumulation and frequency of saturated

180 conditions, thus can be used to predict relative surface wetness and hydrological

181 responses (Meles et al 2020). It is widely used to quantify topographic impact on

182 hydrological processes (i.e., spatial scale effects, hydrological flow path, etc.), as well

183 as in land surface models for hydrological, biogeochemical and ecological processes

184 (Sorensen et al 2006).

185 **2.4 Quantification of the relative importance of soil moisture and precipitation**

186 **during floods**

187 The maximum daily discharge of each year was selected as annual flood, which was

188 then averaged across years as the mean annual maximum flood (AMF). The observed

189 rainfall on that day and the estimated soil water storage at the day before were also

190 averaged across years as daily rainfall ($P$) and antecedent soil moisture ($S_0$). Since

191 almost all the AMFs in our study region come during rainy season when rainfall comes

192 in most of the days. To avoid the bias that may be caused in event separation, the soil

193 moisture at the day before AMF was used as antecedent soil moisture, instead of the

194 day before the event of AMF. To examine the impacts from long-lasting rainfall event,

195 especially for the large watersheds with longer concentration time, we also calculated

196 the mean accumulated rainfall from two days (rainfall on the flood day and the day

197    before, $P_2$) to seven days (weekly rainfall, $P_7$).

198    The percentile of antecedent soil moisture ($S_0$) was calculated to represent the

199    relative saturation of soil moisture in the time series; while the percentile of daily

200    rainfall ($P$) was estimated to show the relative intensity ($P'$), representing the relative

201    magnitude of rainfall in flood generation. The percentile of accumulated rainfall was

202    also calculated for the two-day to seven-day rainfall.

203    To quantify the relative importance of antecedent soil moisture and rainfall in flood

204    generation, the ratio between these two factors at the AMFs was derived: SPR = $S'/P'$.

205    When SPR is large, the antecedent soil moisture is much closer to the maximum, while

206    the daily rainfall is less extreme, floods are more affected by the antecedent soil

207    moisture. On the other hand, a smaller SPR indicates relatively larger magnitude of

208    rainfall comparing with antecedent soil moisture, that is, rainfall is more extreme and

209    influential in flood generation.

210    **3 Results**

211    **3.1 Spatial patterns of antecedent soil moisture and precipitation during floods**

212    Figure 2 shows the spatial distribution of the percentile of antecedent soil moisture and

213    daily rainfall during the annual maximum floods (AMFs) in the middle and lower

214    reaches of the Yangtze River. As we can see from Figure 2a, in the middle and lower

215    reaches of YZRB, when AMFs occurred, the percentile of antecedent soil saturation

216    was generally high, most of them are larger than 0.6: the farther away from the main

217    stream, the more saturated the soil was. On the other hand, along and near the main

218    stream and the delta, the antecedent soil saturation rate could be much smaller, even

219    less than 0.4.

220     Figure 2b shows the daily rainfall during the AMFs. As we can see, the percentile

221     of daily rainfall is relatively high (>0.8) at more than half of the study sites, while it is

222     small (<0.5) for the sites along the main stream and in the delta (Figure 2b). Comparison

223     between Figure 2a and b suggests that, except the sites on the main stream and in the

224     delta, sites with relatively high antecedent soil saturation rate (i.e., >0.8, the blue dots)

225     during AMFs are also the ones with relatively small daily rainfall contribution (i.e.,

226     <0.8, the light blue and cyan dots). That is, for these sites, the AMFs are usually

227     occurring at a near saturated soil condition while extreme rainfall at flood day is not

228     necessary, suggesting the relative importance of soil saturation rate. For the sites with

229     both the percentile of soil moisture and rainfall between 0.6 and 1, both the antecedent

230     soil moisture and rainfall play important roles in flood generation. As for the sites on

231     the main stream and in the delta, both antecedent soil moisture and rainfall are low

232     during AMFs, this is likely due to the regulations from large reservoirs and water gates.

233     **3.2 The scaling effect in the contribution of antecedent soil moisture and rainfall**

234     To further investigate the relative importance of antecedent soil moisture and rainfall

235     in flood generation and the potential influential factors, we examined their correlation

236     with catchment area (Figure 3). Given the complicated environmental and social

237     impacts, the regulated watersheds and sites on the main stream are presented separately

238     (the green dots and cyan dots in Figure 3 respectively). Our study will focus on the sites

239     that are not dominated by regulation (the blue dots in Figure 3), for simplicity, we will

240     refer them as natural watersheds.

241     As we can see from Figure 3, during the occurrence of AMFs, the percentile of

242     antecedent soil saturation increases with watershed area ($p$-value<0.001), while the

243     percentile of daily rainfall decreases with watershed area ($p$-value<0.001). That is, with

244 the increase of watershed size, antecedent soil moisture becomes more and more

245 saturated while the precipitation is less and less extreme during AMFs; suggesting the

246 rising contribution of antecedent soil moisture and declining importance of daily

247 precipitation in flood generation. As for the regulated watersheds (green dots in Figure

248 3), there is no clear correlation between drainage area and the percentile of antecedent

249 soil moisture or rainfall, which is understandable. Meanwhile, both the percentile of

250 antecedent soil moisture and rainfall decreases with watershed area for main stream

251 sites.

252 **3.3 The scaling impacts on accumulated rainfall**

253 The saturation of soil before floods could be due to previous rainfall events, and could

254 also be caused by accumulated rainfall in long-lasting rainfall events that eventually

255 generate floods (Xie et al., 2018). Figure 4 presents the correlation between the

256 percentile of accumulated rainfall and drainage area. When single day rainfall is

257 considered, it is negatively correlated with drainage area (Figure 3a); when

258 accumulated rainfall is considered, the correlation gradually shifts from negative to

259 positive correlation (Figure 4). For example, when two-day rainfall was examined, the

260 correlation between accumulated rainfall and drainage area shifts from negative to

261 positive at 10,000 km$^2$; the negative correlation in Figure 3a is only valid for watersheds

262 larger than 10,000 km$^2$ (Figure 4a). This transition area increases from 10,000 km$^2$ for

263 two-day rainfall to 100,000 km$^2$ for four-day rainfall (Figure 4c). The number of

264 watersheds with negative correlation also decreases. Eventually, the weekly rainfall has

265 similar positive correlation with drainage area like antecedent soil moisture (Figure 4f).

266 The increase of transition area may be explained by the increasing response time and

267 confluence time in large watersheds: it takes days to generate flow events by heavy

268  rainfall and for them to reach outlets where it can be observed in large watersheds. This

269  is also consistent with the conclusion in the Yellow River Basin (Ran et al., 2020) and

270  our previous findings of the dominant flood generation mechanism in the middle and

271  lower YZRB: weekly rainfall is the dominant flood driver for sites on the main streams

272  and the major tributaries (Wang et al 2021). The regulated watersheds don't show

273  significant correlation which is understandable for the strong human intervention. For

274  the negative correlation between accumulated rainfall and drainage area at main stream

275  sites, it is difficult to decide whether it is due to scaling effect or human intervention.

276  **3.4 The interlink of watershed characteristics, flood, antecedent soil moisture and**

277  **rainfall**

278  Figure 5 presents the percentile of antecedent soil moisture and rainfall during the

279  AMFs at the study watersheds, the circles are scaled by watershed size and colored with

280  topographic gradient. Except the watersheds with strong human intervention (regulated

281  ones and the ones on main stream), there is a negative correlation between the

282  contribution of rainfall and antecedent soil moisture. The lower right of the scatter are

283  mostly big blue dots, which are large watersheds with gentle topographic gradient. That

284  is, AMFs usually occur when soil moisture is close to saturation while extreme rainfall

285  is not necessary for AMFs in these watersheds. On top of the scatter are relatively small

286  yellow and green dots, those are medium to small watersheds with steep topographic

287  gradient. That is, AMFs are usually generated with extreme rainfall, while the saturation

288  of soil moisture is not necessary. This negative correlation indicates the shift of

289  dominance in AMFs generation from extreme rainfall to antecedent soil saturation from

290  small steep watersheds to large flat ones.

291  Figure 6 shows the relative importance of antecedent soil moisture and rainfall. For

the natural watersheds (the circles), SPR increases with drainage area and declines with topographic gradient. That is, the larger the drainage area is, the more essential the contribution of antecedent soil moisture to floods is, and the less influential rainfall is in flood generation. For watersheds with similar drainage area (i.e., the green or light blue dots in Figure 6b), topographic gradient also cast impacts on SPR: SPR decreases with slope. That is, the relative importance of rainfall increases at steeper watersheds. This may be attributed to the shortened hydrological response time due to the steep topography which facilitates rainfall induced floods generation. As a combination of both drainage area and topographic gradient, TWI is positively correlated with SPR at natural watersheds, with less scatter than the correlation between SPR and drainage area or topographic gradient alone. That is, watersheds with larger area and gentler topographic gradient that are easier to get wet tend to have larger SPR: soil saturation is more important in flood generation. There is no significant correlation between SPR and TWI for the regulated watersheds along tributaries (black triangles). However, the sites on main stream show opposite pattern: the SPR at these sites decreases with TWI and drainage area. It is difficult to determine whether this is because of reservoir regulation or not. More data about watersheds larger than 10,000km$^2$ but with limited human intervention are needed to examine this hypothesis.

Besides TWI, SPR is also correlated with the magnitude of AMF (Figure 7). As Figure 7 shows, the area normalized flood peak declines with flood-generation SPR. Watersheds with large flood peak are mostly the ones with steep topographic gradient and small SPR (i.e., SPR<1) and *vice versa*. Similar correlation was also found at event scale in our experimental mountainous watershed, which locates at a headwater of Yangtze River (Liu et al 2021).

**4 Discussion**

**4.1 The relative importance of antecedent soil moisture and rainfall in flood generation**

While soil moisture and rainfall are the two main drivers of floods in the middle and lower Yangtze River basin, the dominance of each factor varies across the relatively natural watersheds. Floods in large watersheds are usually generated when soil is almost saturated despite of the relatively small rainfall amount, while extreme rainfall is usually observed during floods in small to medium watersheds (blue dots in Figure 3). The rising contribution of antecedent soil moisture in large watersheds was consistent with the findings in Australian watersheds (Wasko & Nathan, 2019); and the declining influence of rainfall at larger watersheds was also found in Indian watersheds (Garg et al 2019). This contrast correlation with watershed size indicates a shift of dominance in AMFs generation, which may be attributed to the longer confluence time in the large watersheds and less heterogeneity in small watersheds.

This shift of dominance can be observed more straightforward from the negative correlation between the percentile of rainfall and antecedent soil moisture in Figure 5. The natural watersheds in Figure 5 could be grouped into three classes based on their drainage area and topographic gradient. When a watershed is large and flat, flood occurrence is mainly determined by soil saturation (i.e., the big blue dots at the lower right of the scatter); on the other hand, when a watershed is small and steep, heavy rainfall takes over the dominance (i.e., the small yellow and green dots at the upper left of the scatter). Between these two groups are relatively small watersheds with gentle topographic gradient, where the occurrence of AMF requires both highly saturated soil and relatively heavy rainfall. That is, the dominant influential factor(s) in AMFs

340 generation across watersheds is correlated with the topographic characteristics (i.e.,

341 watershed size and topographic gradient). This helps quantify the relative importance

342 of soil moisture and rainfall in flood generation in the existing work.

343 This shift of dominance is not observed in the main stream sites (i.e., cyan dots in

344 Figure 3), where the percentile of both antecedent soil moisture and precipitation

345 declines with drainage area. This may be attributed to the more complicated flood

346 generation mechanism at large scale as well as the strong human intervention on main

347 stream (e.g., reservoirs, water gates regulation, etc.) (Gao et al., 2018; Long et al., 2020;

348 Zhang et al., 2017). The major responsibilities of reservoirs on the main stream are to

349 reduce peak flow and postpone the time to flood peak (Volpi et al., 2018). As a result,

350 the original flood peak would be delayed by regulation and the actual flood peak would

351 occur when rainfall declines/stops and soil water drains. Another possibility is that

352 when watershed size is larger than $100,000km^2$, the impact of antecedent soil moisture

353 declines as well. To examine this hypothesis, more data from watersheds larger than

354 $100,000km^2$ and with limited human intervention is needed. However, this is above the

355 scope of this work and requires future studies.

356 **4.2 Linkage between topographic characteristics, SPR and floods**

357 The correlation between TWI and SPR (Figure 6c) demonstrates that the relative

358 importance of soil moisture and rainfall could be inferred from topographic

359 characteristics quantitatively. We could derive the relative dominance of soil moisture

360 and rainfall in flood generation in specific watershed from its TWI for the natural

361 watersheds without significant human intervention. Rainfall and soil moisture level

362 have been identified as dominant drivers of floods, individually or together, in

363 watersheds worldwide (Berghuijs et al 2016, 2019b; Garg & Mishra 2019; Tramblay et

364 al 2021; Ye et al 2017). Our findings provide a framework to quantify the relative

365 importance of rainfall and soil moisture and to further identify the influential factors of

366 their importance based on topographic characteristics that are easy to measure.

367     Meanwhile, the SPR also present a negative correlation with the magnitude of

368 AMFs (Figure 7). That is, we could infer the mean annual AMF based on SPR for each

369 watershed. Since the characteristic SPR could be estimated from TWI, we could derive

370 quantitative estimation of the mean AMFs from topographic characteristics that are

371 easy to measure, even in watersheds with little hydrologic records. This would be

372 helpful for flood control management in ungauged watersheds, especially in the

373 mountainous watersheds with risks of flash floods. Similar correlation was also found

374 in the observations from our experimental watershed, a headwater of Yangtze River

375 (Liu et al 2021). The ratio of observed antecedent soil moisture and event precipitation

376 also presents similar decline trend with discharge at event scale. However, the

377 correlation between SPR and discharge at event scale is preliminary, more data with

378 higher resolution and detailed analysis are needed for validation at event scale. For this

379 study, our goal is to present the framework to derive flood generation SPR that could

380 be estimated from topographic characteristics and to provide information of mean

381 AMFs.

382     In conclusion, based on the topographic characteristics, we could derive the relative

383 importance of soil moisture and rainfall in flood generation (SPR); and from this

384 relative importance ratio, we could further infer the average flood magnitude at these

385 watersheds. As a result, we could link the topographic characteristics and annual floods

386 through the characteristic SPR during the AMFs.

387 **4.3 Implications**

388 Our findings could be helpful for potential flood risk evaluation in ungauged basins,

389 e.g., headwaters in the mountainous region. With the construction of large reservoirs,

390 the capability of flood risk control has improved substantially along main stream (Zou

391 et al., 2011; Zhang et al., 2015). However, it is still difficult for quantitative evaluation

392 of flood risk in upstream mountainous watersheds, which are vulnerable to floods but

393 difficult for hydrological modeling and prediction due to little hydrologic records.

394 Our findings suggest that we could derive the flood-generation SPR of each

395 watershed from drainage area and topographic gradient that are easy to measure. The

396 correlation between SPR and flood peak provides information of the mean annual

397 floods in ungauged watersheds. Therefore, in regions without observation data, to build

398 flood control infrastructure such as dams and gates, the mean annual flood peak

399 obtained by SPR based on the topographic characteristics can be used to provide

400 quantitative information for flood control and disaster management. Flood control

401 infrastructures could be designed based on the estimated mean annual flood peak as

402 well as the demographic information. With further validation of this framework at event

403 scale, by using the observed soil moisture from remote sensing data and precipitation

404 forecast to generate real-time prediction of SPR values, we could further provide early

405 warning of floods in these ungauged watersheds. But this needs more data and

406 examination in future studies.

407 **4.4 Limitations**

408 Previous works usually identify the dominant flood generation mechanism based on the

409 comparison of the timing of events (Berghuijs et al 2016; 2019b; Bloschl et al 2017; Ye

410 et al 2017). Similar work has been implemented in our study watersheds, suggesting

411 the importance of soil moisture and rainfall (Wang et al 2021). Based on that, we further

412   looked into the records to quantitatively evaluate the relative importance of soil

413   moisture and rainfall in flood generation. However, there are limitations in our methods.

414   The precipitation data we used were averaged for the study watersheds from 247

415   meteorological stations. Given the large area and considerable spatial heterogeneity, the

416   precipitation data we used may not always be representative of the actual precipitation

417   events. The daily data could also average the rainfall intensity at hourly scale, which

418   could be influential in small mountainous watersheds. ET was scaled as $0.75*ET_0$ to

419   make sure it is smaller than the potential evaporation. This is a simplified estimation of

420   ET; more sophisticated method is needed in further analysis on specific catchments at

421   event scale.

422   The estimation of soil moisture is also highly simplified, which cannot be

423   considered as precise estimation at event scale. To reduce the influence from this

424   simplification, we used the percentile of soil moisture to represent the relative saturation

425   of soil moisture as well as the seasonal trend of soil moisture, which was then compared

426   with the percentile of rainfall. While more sophisticated models can be used for soil

427   moisture estimation, there could still be substantial uncertainties (Zaherpour et al., 2018;

428   Ran et al 2020). Yet the seasonal trend and the relative magnitude, after averaging

429   through long-term records would be less impacted by the simplification in estimation

430   (Berghuijs et al 2019; Zhang et al 2019).

431   It is possible that soil moisture at the day before the AMFs may not be the soil

432   moisture before event in large catchments due to the long concentration time. We

433   estimated the concentration time for 10 sites with largest drainage area (larger than

434   100,000 km²): the ones on the main stream and at the outlets of major tributaries

435   following the USBR method (USBR 1973; Gericke & Smithers 2014). The

concentration time is mostly within two days for main stream sites and is less than 24hr for sites at the outlets of major tributaries (Table S1). Since the rest of the sites are all smaller than these ones, so would be the concentration time. That is, for the natural watersheds we focused on, the concentration time is likely to be within one day. Thus, the soil moisture at the day before AMFs would contribute to the generation of AMFs, and should be applicable for this study.

Besides, the exchange with groundwater was not considered in the soil moisture estimation. The exchange with groundwater is more complicated and heterogenous (i.e., rivers could receive groundwater recharge in hilly area and recharge groundwater in lower land (Che et al 2021)). According to Huang et al. (2021), the variation of groundwater level in the Yangtze River basin is relatively small. Since the goal of this study is to capture the first order seasonal variation of soil moisture and develop a framework that differentiates the relative importance of precipitation and soil moisture in flood generation, in this study, we estimated the soil moisture following Berhuijs (et al 2016, 2019) with a simple water balance equation.

Moreover, this work is focused on the relative importance soil moisture and rainfall, the impact of snowmelt is not considered due to the warm and humid climate in the study watersheds. To apply our findings to cold watersheds with significant impact of snow, the snowmelt component needs to be incorporated. In addition, our method is based on the average values from many years. While previous work indicated that the occurrence of floods in our study watersheds are highly concentrated (Wang et al 2021), there could be strong inter-annual variability in other watersheds. In future studies, annual scale and event scale analysis are needed to examine and improve our findings before it can be applied to watersheds with more diverse climate and landscape

460 conditions. more comprehensive models with sophisticated groundwater component,

461 remote sensing data, and reanalysis product with higher spatial-temporal resolution are

462 needed to provide more accurate estimation of soil moisture, ET, and refine the

463 estimation of the flood-generation SPR.

464 **5 Conclusions**

465 Heavy rainfall on highly saturated soil was identified as the dominant flood generation

466 mechanism across world (Berghuijs et al 2019; Wang et al 2021; Wasko et al 2020).

467 This study aims to further evaluate the relative importance of antecedent soil moisture

468 and rainfall on floods generation and the controlling factors. Climate and hydrological

469 data from 224 hydrological stations and 247 meteorological stations in the middle and

470 lower reaches of the Yangtze River basin was analyzed, along with the modeled soil

471 moisture. Except the regulated watersheds, the relative importance of antecedent soil

472 moisture and daily rainfall present significant correlation with drainage area: the larger

473 the watershed is, the more essential antecedent soil saturation rate is in flood generation,

474 the less important daily rainfall is.

475 Using the percentile of antecedent soil moisture and rainfall as coordinates, the

476 flood generation mechanism(s) of study watersheds could be grouped into three classes:

477 antecedent soil moisture dominated large flat watersheds, heavy rainfall dominated

478 steep and small to middle size watersheds, and small to middle size watersheds with

479 gentle topographic gradient where floods occurrence requires both highly saturated soil

480 and heavy rainfall. Our analysis further shows that the ratio of relative importance

481 between antecedent soil moisture and rainfall (SPR) can be predicted by topographic

482 wetness index. When the topographic wetness index is large, the dominance of

483 antecedent soil moisture for extreme floods is stronger, and *vice versa*. The SPR also

484      presents negative correlation with area normalized flood peak.

485      With the potential increase of extreme rainfall events (Gao et al., 2016; Chen et

486      al., 2016), upstream mountainous watersheds in the middle and lower Yangtze River

487      basin are facing higher risk of extreme floods. The lack of hydrological records further

488      increases the vulnerability of people in these watersheds. The flood risks could be

489      reduced by construction of flood control facilities, but it is difficult to set flood control

490      standards in these ungauged watersheds. Our findings provide a framework to

491      quantitatively estimate the possible flood risk for these ungauged watersheds. Based on

492      measurable watershed characteristics (i.e., drainage area and topographic gradient), the

493      flood generation SPR could be derived, which could then be used to estimate the mean

494      annual flood. This information can provide scientific support for flood control

495      management as well as infrastructures construction.

496      Future analysis at event scale could help generate the flood-generation curve

497      between SPR and discharge at event scale to further improve flood risk predictions in

498      these small ungauged watersheds. With more data from other regions and improved

499      estimation or observation of soil moisture, we could expand our analysis to watersheds

500      with more diverse climate and topographic characteristics to examine and refine our

501      findings and to enhance our understandings of flood generation.

502

503      **Data availability**

504      DEM data was downloaded from Geospatial Data Cloud at http://www.gscloud.cn/.

505      Climatological data used in this study was obtained from China Meteorological Data

506      Network, which can be accessed at http://data.cma.cn/. Discharge data comes from

507      Annual Hydrological Report of the People's Republic of China issued by Yangtze River

508      Water Resources Commission.

509

**Acknowledgements**

This research was funded by the National Key Research and Development Program of China (2019YFC1510701-01), and National Natural Science Foundation of China (51979243).

**References**

Abbas, S.A., Xuan, Y. and Song, X.: Quantile Regression Based Methods for Investigating Rainfall Trends Associated with Flooding and Drought Conditions. Water Resources Management, 33(12), 4249-4264, https://doi:10.1007/s11269-019-02362-0, 2019.

Alfonso R., Nilza M. R.C., and Anderson L. R.: Numerical Modelling of the Topographic Wetness Index: An Analysis at Different Scales, International Journal of Geosciences(4), 476-483, https:// doi:10.4236/ijg.2011.24050, 2011.

Allen R. G., Pereira L. S. and Races D.: Crop evapotranspiration-Guidelines for computing crop water requirements FAO Irrigation and drainage paper NO.56(Electric Publication)[M], Rome , Italy:FAO, 1998.

Bennett, B., Leonard, M., Deng, Y., Westra, S.: An empirical investigation into the effect of antecedent precipitation on flood volume. J. Hydrol. 567, 435–445. https://doi.org/10.1016/j.jhydrol.2018.10.025, 2018.

Berghuijs, W.R., Allen, S.T., Harrigan, S. and Kirchner, J.W.: Growing Spatial Scales of Synchronous River Flooding in Europe. Geophysical Research Letters, 46(3), 1423-1428, https://doi:10.1029/2018GL081883, 2019a.

Berghuijs, W.R., Harrigan, S., Molnar, P., Slater, L.J. and Kirchner, J.W.: The Relative Importance of Different Flood-Generating Mechanisms Across Europe. Water Resources Research, 55(6), 4582-4593, https://doi:10.1029/2019WR024841, 2019b.

Berghuijs, W.R., Woods, R.A., Hutton, C.J. and Sivapalan, M.: Dominant flood generating mechanisms across the United States. Geophysical Research Letters, 43(9), 4382-4390, https://doi:10.1002/2016GL068070, 2016.

Bertola, M., Viglione, A., Vorogushyn, S., Lun, D., Merz, B., Blöschl, G.: Do small and large floods have the same drivers of change? A regional attribution analysis in Europe. Hydrol. Earth Syst. Sci. 25, 1347–1364. https://doi.org/10.5194/hess-25-1347-2021, 2021.

543   Bloschl, G., Nester, T., Komma, J., Parajka, J. and Perdigao, R.A.P.: The June 2013
544         flood in the Upper Danube Basin, and comparisons with the 2002, 1954, and 1899
545         floods. Hydrol. Earth Syst. Sci., 17, 5197–5212, 2013.

546   Blöschl, G., Hall, J., Parajka, J., Perdigão, R. A., Merz, B., Arheimer, B., et al.:
547         Changing climate shifts timing of European floods. Science, 357(6351), 588–
548         590. https://doi.org/10.1126/science.aan2506, 2017.

549   Bloschl, G., Hall, J., Viglione, A., Perdigao, R.A., Parajka, J., Merz, B., et al.: Changing
550         climate both increases and decreases European river floods, Nature, 573, 108 –
551         111, 2019.
552   Berti, A., Tardivo, G., Chiaudani, A., Rech, F. and Borin, M.: Assessing reference
553         evapotranspiration by the Hargreaves method in north-eastern Italy. Agricultural
554         Water Management, 140, 20-25, https://doi:10.1016/j.agwat.2014.03.015, 2014.

555   Brunner, M. I., Seibert, J. and Favre, A.C.: Bivariate return periods and their importance
556         for flood peak and volume estimation. Wire's Water, 3, 819 – 833.
557         https://doi.org/10.1002/wat2.1173, 2016.

558   Brunner, M. I., Gilleland, E., Wood, A., Swain, D. L., and Clark, M.: Spatial
559         dependence of floods shaped by spatiotemporal variations in meteorological and
560         land - surface processes. Geophysical Research Letters, 47, e2020GL088000.
561         https://doi.org/ 10.1029/2020GL088000, 2020.

562   Brunner, M. I., Swain, D. L., Wood, R.R. et al. An extremeness threshold determines
563         the regional response of floods to changes in rainfall extremes. Commun Earth
564         Environ 2, 173. https://doi.org/10.1038/s43247-021-00248-x, 2021.

565   Cai, Q. H.: Great protection of Yangtze River and watershed ecology, Yangtze River
566         (01), 70-74, https://doi:10.16232/j.cnki.1001-4179.2020.01.011, 2020.

567   Cen, S.-x., Gong, Y.-f., Lai, X. and Peng, L.: The Relationship between the
568         Atmospheric Heating Source/Sink Anomalies of Asian Monsoon and

Flood/Drought in the Yangtze River Basin in the Meiyu Period. Journal of Tropical Meteorology, 21(4), 352-360, 2015.

Che, Q., Su, X., Zheng, S., Li, Y.: Interaction between surface water and groundwater in the Alluvial Plain (anqing section) of the lower Yangtze River Basin: environmental isotope evidence. Journal of Radioanalytical and Nuclear Chemistry, 329, 1331–1343, 2021.

Chen, Y. and Zhai, P.: Mechanisms for concurrent low-latitude circulation anomalies responsible for persistent extreme precipitation in the Yangtze River Valley. Climate Dynamics,47(3-4), 989-1006, https://doi:10.1007/s00382-015-2885-6, 2016.

CRED (2015). The human cost of natural disasters: A gobal perspective: Centre for research on the epidemiology of disasters.

Deb, P., Kiem, A.S. and Willgoose, G.: Mechanisms influencing non-stationarity in rainfall-runoff relationships in southeast Australia. Journal of Hydrology, 571, 749-764, https://doi:10.1016/j.jhydrol.2019.02.025, 2019.

Desai, B., Maskrey, A., Peduzzi, P., De Bono, A., & Herold, C. Making Development Sustainable: The Future of Disaster Risk Management. Global Assessment Report on Disaster Risk Reduction http://archive-ouverte.unige.ch/unige:78299 (UNISDR, 2015).

Do, H. X., Mei, Y., & Gronewold, A. D.: To what extent are changes in flood magnitude related to changes in precipitation extremes? Geophysical Research Letters, 47, e2020GL088684. https://doi.org/10.1029/2020GL088684, 2020.

Fang, X. and Pomeroy, J.W.: Impact of antecedent conditions on simulations of a flood in a mountain headwater basin. Hydrological Processes, 30(16), 2754-2772, https://doi:10.1002/hyp.10910, 2016.

Feng, B. F., Dai M. L. and Zhang T.: Effect of Reservoir Group Joint Operation on Flood Control in the Middle and Lower Reaches of Yangtze River, Journal of Water Resources Research (3), 278-284, https://doi:10.12677/JWRR.2017.63033, 2017.

Fu, G., Yu, J., Yu, X., Ouyang, R., Zhang, Y., Wang, P., Liu, W. and Min, L.: Temporal variation of extreme rainfall events in China, 1961-2009. Journal of Hydrology, 487, 48-59, https://doi:10.1016/j.jhydrol.2013.02.021, 2013.

601  Gao, T. and Xie, L.: Spatiotemporal changes in precipitation extremes over Yangtze
602      River basin, China, considering the rainfall shift in the late 1970s. Global and
603      Planetary Change, 147, 106-124, https://doi:10.1016/j.gloplacha.2016.10.016,
604      2016.

605  Gao, Y., Wang, H., Lu, X., Xu, Y., Zhang, Z. and Schmidt, A.R.: Hydrologic Impact
606      of Urbanization on Catchment and River System Downstream from Taihu Lake.
607      Journal of Coastal Research, 82-88, https://doi:10.2112/SI84-012.1, 2018.

608  Garg, S., & Mishra, V.: Role of extreme precipitation and initial hydrologic conditions
609      on floods in Godavari river basin, India. Water Resources Research, 55, 9191–
610      9210. https://doi.org/10.1029/2019WR025863, 2019.

611  Grabs, T., Seibert, J., Bishop, K. and Laudon, H.: Modeling spatial patterns of saturated
612      areas: A comparison of the topographic wetness index and a dynamic distributed
613      model.      Journal      of      Hydrology,      373(1-2),      15-23,
614      https://doi:10.1016/j.jhydrol.2009.03.031, 2009.

615  Huang, C., Zhou, Y., Zhang, S., Wang, J., Liu, F., Gong, C., Yi, C., Li, L., Zhou, H.,
616      Wei, L., Pan, X., Shao, C., Li, Y., Han, W., Yin, Z., and Li, X.: Groundwater
617      resources in the Yangtze River Basin and its current development and utilization[J].
618      Geology of China, 2021, 48(4):979-1000.

619  IPCC. Managing the Risks of Extreme Events and Disasters to Advance Climate
620      Change Adaptation (eds Field, C. B. et al.) (Cambridge Univ. Press, 2012).

621  Kato, K.: On the Abrupt Change in the Structure of the Baiu Front over the China
622      Continent in Late May of 1979. Journal of the Meteorological Society of Japan,
623      63(1), 20-36, https://doi:10.2151/jmsj1965.63.1_20, 1985.

624  Kazuki, T., Oliver C. S. V., Masahiro, R.: Spatial variability of precipitation and soil
625      moisture on the 2011 flood at chao phraya river basin.International Water
626      Technology Association, Proceedings of Hydrology and Water Resources, B, 17-
627      21, 2013.

628  Kemter, M., Merz, B., Marwan, N., Vorogushyn, S., & Blöschl, G.: Joint trends in flood
629      magnitudes and spatial extents across Europe. Geophysical Research Letters, 47,
630      e2020GL087464. https://doi.org/10.1029/2020GL087464, 2020.

631  Lehner, B., C. Reidy Liermann, C. Revenga, C. Vörösmarty, B. Fekete, P. Crouzet, P.
632      Döll, M. Endejan, K. Frenken, J. Magome, C. Nilsson, J.C. Robertson, R. Rodel,
633      N. Sindorf, and D. Wisser. 2011. High-resolution mapping of the world's

634    reservoirs and dams for sustainable river-flow management. Frontiers in Ecology
635    and the Environment 9 (9): 494-502.

636  Li, Q., Wei, F. and Li, D.: Interdecadal variation of East Asian summer monsoon and
637    drought/flood distribution over eastern China in the last 159 years. Journal of
638    Geographical Sciences, 21(4), 579-593, https://doi:10.1007/s11442-011-0865-2,
639    2011.

640  Li, X., Zhang, K., Gu, P., Feng, H., Yin, Y., Chen, W. and Cheng, B.: Changes in
641    precipitation extremes in the Yangtze River Basin during 1960-2019 and the
642    association with global warming, ENSO, and local effects. Science of the Total
643    Environment, 760, https://doi:10.1016/j.scitotenv.2020.144244, 2021.

644  Liu, B., Yan, Y., Zhu, C., Ma, S., & Li, J.: Record-breaking Meiyu rainfall around the
645    Yangtze River in 2020 regulated by the subseasonal phase transition of the North
646    Atlantic Oscillation. Geophysical Research Letters, 47, e2020GL090342.
647    https://doi. Org/10.1029/2020GL090342, 2020.

648  Liu, L., Ye, S., Chen, C., Pan, H. and Ran, Q.: Nonsequential Response in Mountainous
649    Areas of Southwest China. Frontiers in Earth Science, 9: 1-15. doi:
650    10.3389/feart.2021.660244, 2021

651  Liu, N., Jin, Y. and Dai, J.: Variation of Temperature and Precipitation in Urban
652    Agglomeration and Prevention Suggestion of Waterlogging in Middle and Lower
653    Reaches of Yangtze River. 3$^{rd}$ International Conference on Energy Equipment
654    Science and Engineering (Iceese 2017), 128, https://doi:10.1088/1755-
655    1315/128/1/012165, 2018.

656  Liu, S., Huang, S., Xie, Y., Wang, H., Leng, G., Huang, Q., Wei, X., and Wang, L.:
657    Identification of the Non-stationarity of Floods: Changing Patterns, Causes, and
658    Implications, Water Resour. Manag., 33, 939–953, 2018.

659  Liu, Y., Xinyu, L., Liancheng, Z., Yang, L., Chunrong, J., Ni, W. and Juan, Z.:
660    Quantifying rain, snow and glacier meltwater in river discharge during flood
661    events in the Manas River Basin, China. Natural Hazards, 108(1), 1137-1158,
662    https://doi:10.1007/s11069-021-04723-8, 2021.

663  Long, L.H., Ji, D.B., Yang, Z.Y., Cheng, H.Q., Yang, Z.J., Liu, D.F., Liu, L. and Lorke,
664    A.: Tributary oscillations generated by diurnal discharge regulation in Three
665    Gorges Reservoir. Environmental Research Letters, 15(8),
666    https://doi:10.1088/1748-9326/ab8d80, 2020.

667 Lu, M., Wu, S.-J., Chen, J., Chen, C., Wen, Z. and Huang, Y.: Changes in extreme
668     precipitation in the Yangtze River basin and its association with global mean
669     temperature and ENSO. International Journal of Climatology, 38(4), 1989-2005,
670     https://doi:10.1002/joc.5311, 2018.

671 Meles, M.B., Younger, S.E., Jackson, C.R., Du, E., Drover, D.: Wetness index based
672     on landscape position and topography (WILT): Modifying TWI to reflect
673     landscape position, Journal of Environmental Management 255, 109863, 2020.

674 Miao, Q., Huang, M. and Li, R., Q.: Response of net primary productivity of vegetation
675     in Yangtze River Basin to future climate change. Journal of Natural Resources, 25,
676     08(2010):1296-1305, doi:CNKI:SUN:ZRZX.0.2010-08-007, 2015.

677 Munoz, S.E., Giosan, L., Therrell, M.D., Remo, J.W.F., Shen, Z., Sullivan, R.M.,
678     Wiman, C., O'Donnell, M., and Donnelly, J.P.: Climatic control of Mississippi
679     River flood hazard amplified by river engineering, 556, 95 – 98, 2018.

680 Musselman, K.N., Lehner, F., Ikeda, K., Clark, M.P., Prein, A.F., Liu, C., Barlage, M.
681     and Rasmussen, R.: Projected increases and shifts in rain-on-snow flood risk over
682     western North America, Nature Climate Change, 8, 808 – 812, 2018.

683 Ockert J. G. and Jeff C. S.: Review of methods used to estimate catchment response
684     time for the purpose of peak discharge estimation, Hydrological Sciences Journal,
685     59:11, 1935-1971, DOI: 10.1080/02626667.2013.866712, 2014.

686 Ohmura, A. and Wild, M.: Is the hydrological cycle accelerating? Science, 298, 1345–
687     1346, 2002.

688 Pegram, G. and Bardossy, A.: Downscaling Regional Circulation Model rainfall to
689     gauge sites using recorrelation and circulation pattern dependent quantile-quantile
690     transforms for quantifying climate change. Journal of Hydrology, 504, 142-159,
691     https://doi:10.1016/j.jhydrol.2013.09.014, 2013.

692 Peng, T., Tian, H., Singh, V. P., Chen, M., Liu, J., Ma, H. B. and Wang, J. B.:
693     Quantitative assessment of drivers of sediment load reduction in the Yangtze River
694     basin,           China,           Journal           of           Hydrology,           580,
695     https://doi:10.1016/j.jhydrol.2019.124242, 2020.

696 Qian, H. and Xu, S.-B.: Prediction of Autumn Precipitation over the Middle and Lower
697     Reaches of the Yangtze River Basin Based on Climate Indices. Climate, 8(4),
698     https://doi:10.3390/cli8040053, 2020.

699     Ran, Q., Chen, X., Hong Y., Ye S., and Gao J.: Impacts of terracing on hydrological
700         processes: A case study from the Loess Plateau of China. Journal of Hydrology,
701         588, https:// doi:10.1016/j.jhydrol.2020.125045, 2020.

702     Ran, Q., Zong, X., Ye, S., Gao, J. and Hong, Y.: Dominant mechanism for annual
703         maximum flood and sediment events generation in the Yellow River basin. Catena,
704         187, https://doi:10.1016/j.catena.2019.104376, 2020.

705     Ray S. M., Ramakar J. and Kishanjit K. K.: Precipitation-runoff simulation for a
706         Himalayan River Basin, India using artificial neural network algorithms, Sciences
707         in Cold and Arid Regions, 5(1), 85-95, 2013.

708     Rottler, E., Francke, T., Burger, G., and Bronstert, A.: Long-term changes in central
709         European river discharge for 1869−2016: impact of changing snow covers,
710         reservoir constructions and an intensified hydrological cycle, Hydrol. Earth Syst.
711         Sci., 24, 1721−1740, 2020.

712     Smith, J. A., Cox, A. A., Baeck, M. L., Yang, L., and Bates, P.: Strange floods: the
713         upper tail of flood peaks in the United States, Water Resour. Res., 54, 6510−6542,
714         2018.

715     Sorensen, R., Zinko, U., and Seibert, J.: On the calculation of the topographic wetness
716         index: evaluation of different methods based on field observations, Hydrology and
717         Earth System Sciences, 10, 101−112, 2006.

718     Su, Z., Ho, M., Hao, Z., Lall, U., Sun, X., Chen, X. and Yan, L.: The impact of the
719         Three Gorges Dam on summer streamflow in the Yangtze River Basin.
720         Hydrological Processes, 34(3), 705-717, https://doi:10.1002/hyp.13619, 2020.

721     Suresh, S. S., Benefit O., Augustine T., and Trevor P. : Peoples' Perception on the
722         Effects of Floods in the Riverine Areas of Ogbia Local Government Area of
723         Bayelsa State, Nigeria, Knowledge Management, https://doi:10.18848/2327-
724         7998/CGP/v12i02/50793, 2013.

725     Tao, S. Y., Rainstorm in China [M], Beijing: Science Press, 1980.(in Chinese)

726     Tramblay, Y., Villarini, G., El Khalki, E. M., Gründemann, G., & Hughes, D.:
727         Evaluation of the drivers responsible for flooding in Africa. Water Resources
728         Research, 57, e2021WR029595. https://doi. Org/10.1029/2021WR029595, 2021.

729  USBR (United States Bureau of Reclamation), 1973. Design of small dams. 2nd ed.
730       Washington, DC: Water Resources Technical Publications.

731  Vicente-Serrano, S.M., Azorin-Molina, C., Sanchez-Lorenzo, A., Revuelto, J., Lopez-
732       Moreno, J.I., Gonzalez-Hidalgo, J.C., Moran-Tejeda, E. and Espejo, F.: Reference
733       evapotranspiration variability and trends in Spain, 1961-2011. Global and
734       Planetary Change, 121, 26-40, https://doi:10.1016/j.gloplacha.2014.06.005, 2014.

735  Volpi, E., Di Lazzaro, M., Bertola, M., Viglione, A. and Fiori, A.: Reservoir Effects on
736       Flood Peak Discharge at the Catchment Scale. Water Resources Research, 54(11),
737       9623-9636, https://doi:10.1029/2018wr023866, 2018.

738  Wang, H., Zhou, Y., Pang, Y. and Wang, X.: Fluctuation of Cadmium Load on a Tide-
739       Influenced Waterfront Lake in the Middle-Lower Reaches of the Yangtze River.
740       Clean-Soil Air Water, 42(10), 1402-1408, https://doi:10.1002/clen.201300693,
741       2014.

742  Wang, J., Ran, Q., Liu, L., Pan, H. and Ye, S.: Study on the Dominant Mechanism of
743       Extreme Flow Events in the Middle and Lower Reaches of the Yangtze River,
744       China Rural Water and Hydropower, Accepted.

745  Wang, R., Yao, Z., Liu, Z., Wu, S., Jiang, L. and Wang, L.: Snow cover variability and
746       snowmelt in a high-altitude ungauged catchment. Hydrological Processes, 29(17),
747       3665-3676, https://doi:10.1002/hyp.10472, 2015.

748  Wang, W., Xing W., Yang, T., Shao, Q., Peng, S., Yu, Z., and Yong, B.: Characterizing
749       the changing behaviours of precipitation concentration in the Yangtze River Basin,
750       China. Hydrological Processes, 27(24), 3375-3393, https://doi: 10.1002/hyp.9430,
751       2013.

752  Wang, Z. and Plate, E.: Recent flood disasters in China. Proceedings of the Institution
753       of Civil Engineers – Water and Maritime Engineering (3),
754       https://doi:10.1680/wame.2002.154.3.177, 2002.

755  Wasko, C. and Nathan, R.: Influence of changes in rainfall and soil moisture on trends
756       in flooding. Journal of Hydrology, 575, 432-441,
757       https://doi:10.1016/j.jhydrol.2019.05.054, 2019.

758  Wasko, C., Nathan, R., & Peel, M. C.: Changes in antecedent soil moisture modulate
759       flood seasonality in a changing climate. Water Resources Research, 56,
760       e2019WR026300. https:// doi.org/10.1029/2019WR026300, 2020.

Wasko, C., Nathan, R., Stein, L., O'Shea, D.: Evidence of shorter more extreme rainfalls and increased flood variability under climate change. J. Hydrol. 603, 126994. https://doi.org/10.1016/j.jhydrol.2021.126994, 2021.

Wu, X. S., Guo, S. L. and Ba, H. H.: Long-term precipitation forecast method based on SST multipole index, Journal of water conservancy(10), 1276-1283, https://doi:10.13243/j.cnki.slxb.20180544, 2018.

Xia, J. and Chen, J.: A new era of flood control strategies from the perspective of managing the 2020 Yangtze River flood. Science China-Earth Sciences, 64(1), 1-9, https://doi:10.1007/s11430-020-9699-8, 2021.

Xie, Z., Du, Y., Zeng, Y. and Miao, Q.: Classification of yearly extreme precipitation events and associated flood risk in the Yangtze-Huaihe River Valley. Science China-Earth Sciences, 61(9), 1341-1356, https://doi:10.1007/s11430-017-9212-8, 2018.

Yang, H.F., Yang, S.L., Xu, K.H., Milliman, J.D., Wang, H., Yang, Z., Chen, Z. and Zhang, C.Y.: Human impacts on sediment in the Yangtze River: A review and new perspectives. Global and Planetary Change, 162, 8-17, https://doi:10.1016/j.gloplacha.2018.01.001, 2018.

Yang, L., Wang, L., Li, X. and Gao, J.: On the flood peak distributions over China. Hydrology and Earth System Sciences, 23(12), 5133-5149, https://doi:10.5194/hess-23-5133-2019, 2019.

Yang, W., Yang, H., and Yang, D.: Classifying floods by quantifying driver contributions in the Eastern Monsoon Region of China, Journal of Hydrology, 585, 124767, 2020.

Yang, W., Yang, H., Yang, D., and Hou, A.: Causal effects of dams and land cover changes on flood changes in mainland China. Hydrol. Earth Syst. Sci., 25, 2705–2720, 2021.

Ye, S., Li, H., Leung, L.R., Guo, J., Ran, Q., Demissie, Y., et al., 2017. Understanding flood seasonality and its temporal shifts within the contiguous United States. J. Hydrometeorol. 18 (7), 1997–2009.

Ye, X., Xu, C.-Y., Li, Y., Li, X. and Zhang, Q.: Change of annual extreme water levels and correlation with river discharges in the middle-lower Yangtze River: Characteristics and possible affecting factors. Chinese Geographical Science,27(2), 325-336, https://doi:10.1007/s11769-017-0866-x, 2017.

794 Yu, F., Chen, Z., Ren, X. and Yang, G.: Analysis of historical floods on the Yangtze
795 River, China: Characteristics and explanations. Geomorphology,113(3-4), 210-
796 216, https://doi:10.1016/j.geomorph.2009.03.008, 2009.

797 Zaherpour, J., Gosling, S. N., Mount, N., Schmied, H. M., Veldkamp, T. I., et
798 al. :Worldwide evaluation of mean and extreme runoff from six global-scale
799 hydrological models that account for human impacts. Environmental Research
800 Letters, 13(6), 065015. https://doi. org/10.1088/1748-9326/aac547, 2018.

801 Zhang, H., Liu, S., Ye, J. and Yeh, P.J.F.: Model simulations of potential contribution
802 of the proposed Huangpu Gate to flood control in the Lake Taihu basin of China.
803 Hydrology and Earth System Sciences, 21(10), 5339-5355,
804 https://doi:10.5194/hess-21-5339-2017, 2017.

805 Zhao, J., Li, J., Yan, H., Zheng, L. and Dai, Z.: Analysis on the Water Exchange
806 between the Main Stream of the Yangtze River and the Poyang Lake. 2011 3rd
807 International Conference on Environmental Science and Information Application
808 Technology Esiat 2011, Vol 10, Pt C,10, 2256-2264,
809 https://doi:10.1016/j.proenv.2011.09.353, 2011.

810 Zhang, S., Kang, L. and He, X.: Equal proportion flood retention strategy for the leading
811 multireservoir system in upper Yangtze River. International Conference on Water
812 Resources and Environment, WRE 2015, 2015.

813 Zhang, W., Villarini, G., Vecchi, G.A. and Smith, J. A.: Urbanization exacerbated the
814 rainfall and flooding caused by hurricane Harvey in Houston. Nature, 563, 384 –
815 388, 2018.

816 Zhang, K., Wang, Q., Chao, L., Ye, J., Li, Z., Yu, Z., Yang, T. and Ju, Q.: Ground
817 observation-based analysis of soil moisture spatiotemporal variability across a
818 humid to semi-humid transitional zone in China. Journal of Hydrology, 574, 903-
819 914, 2019.

820 Zou, B., Li, Y., Feng, B.: Analysis on dispatching influence of Three Gorges Reservoir
821 on water level of main stream in mid-lower reaches of Yangtze River: a case study
822 of flood in July,2010. Yangtze River, 42.06:80-82+100. doi:10.16232/j.cnki.1001-
823 4179.2011.06.004, 2011.

824
825
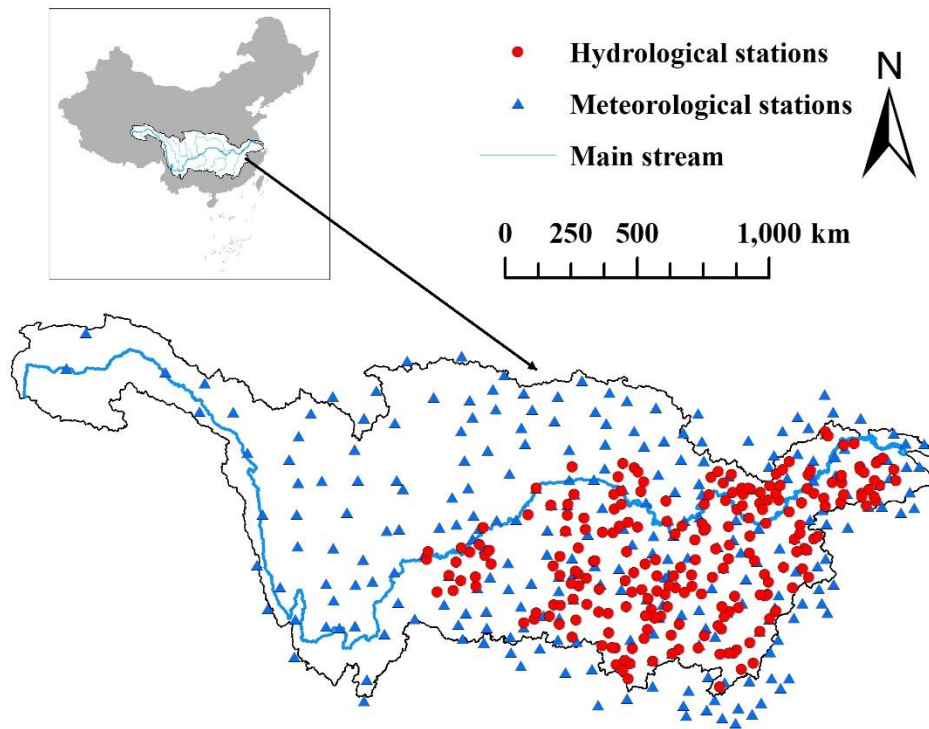
826

827 **Figure 1**: Map of the Yangtze River basin, and the meteorological stations and

828 hydrological stations. The blue line is the main stream of Yangtze River.

829
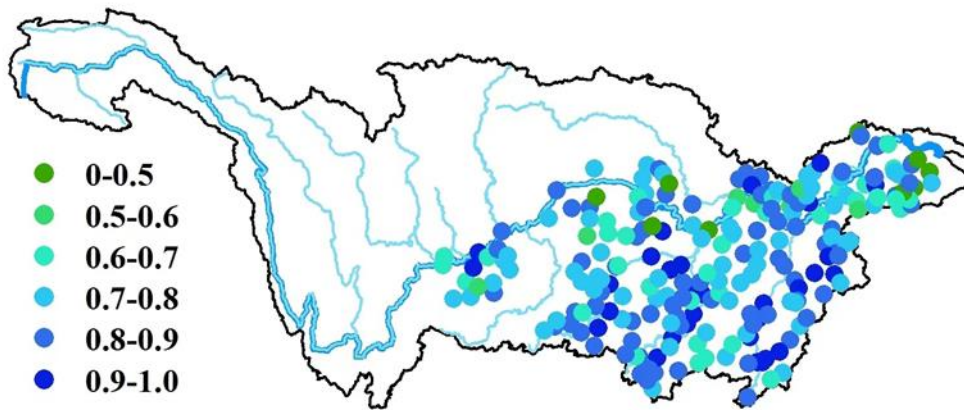
(a)Percentile of antecedent soil moisture
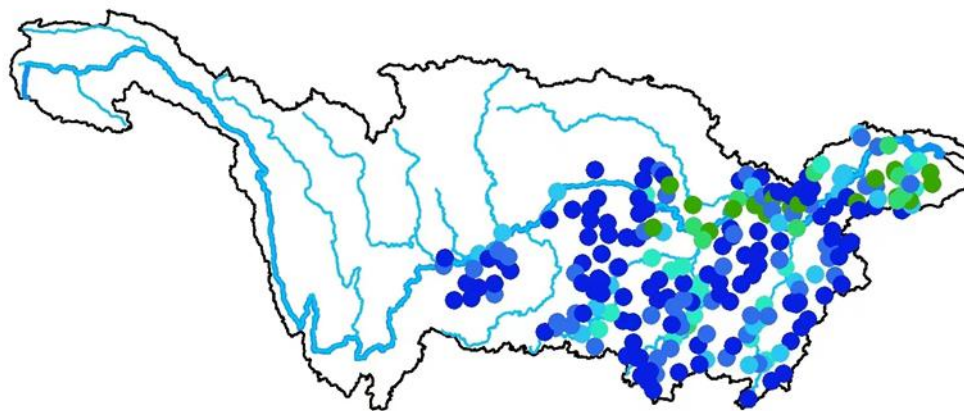
(b)Percentile of precipitation

830

831  **Figure 2**: The spatial distribution of (a) the percentile of antecedent soil moisture during

832  annual maximum flood; (b) the percentile of daily precipitation during annual

833  maximum flood.

834
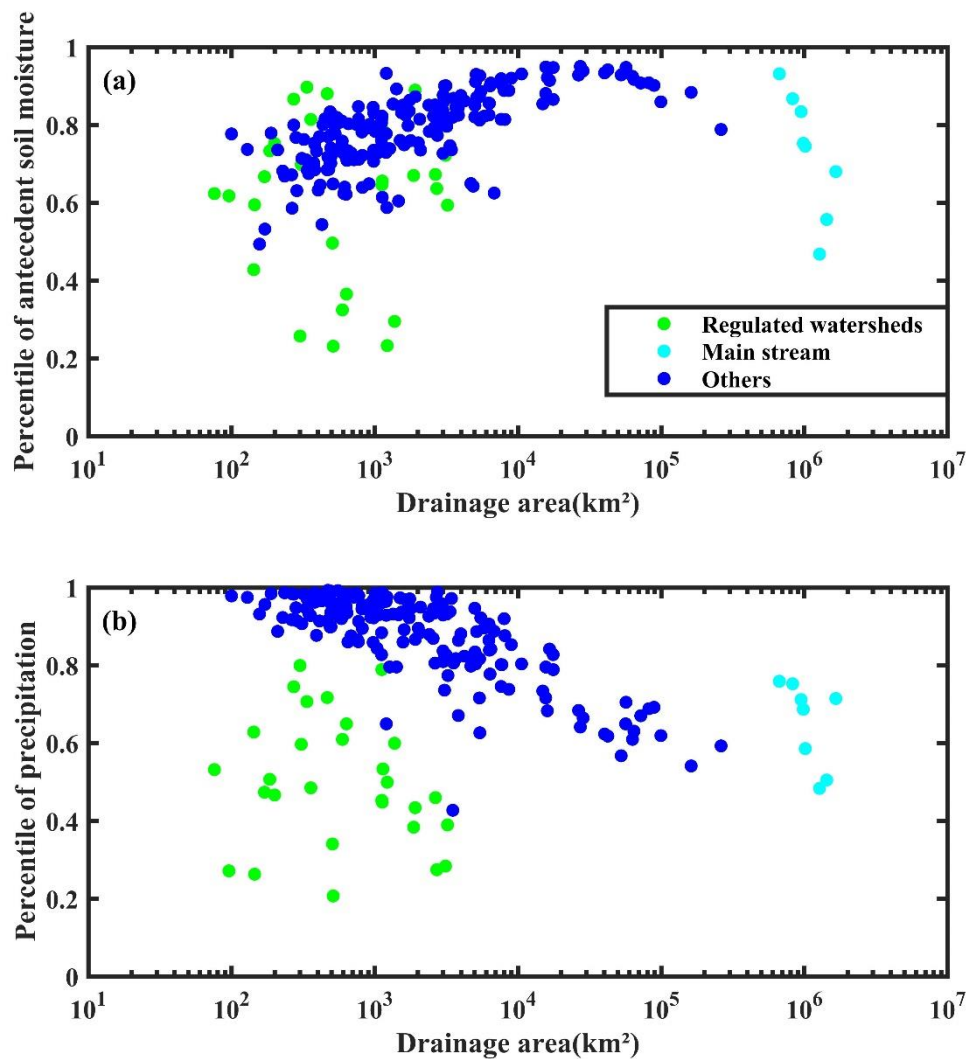
835

836 **Figure 3**: Scatterplot between the drainage area and (a) the percentile of antecedent soil

837 moisture of AMF events (the linear regression for blue dots: $R^2 = 0.46$, *p*-value<0.001);

838 (b) the percentile of precipitation at the day of AMF events (the linear regression for

839 blue dots: $R^2 = 0.61$, *p*-value<0.001). The green dots represent the regulated watershed,

840 the cyan dots represent the sites on the main stream, and the rest sites are shown in blue.

841

842

843
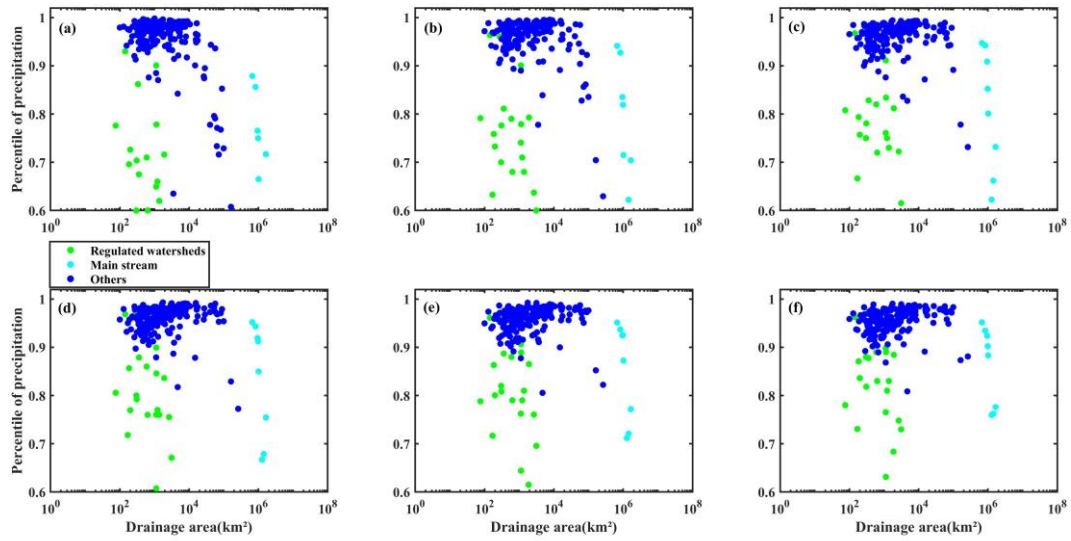
844

845 **Figure 4**: Scatterplot between the drainage area and the percentile of accumulated

846 rainfall of (a) two days; (b) three days; (c) four days; (d) five days; (e) six days; and (f)

847 seven days on AMF events.

848

849
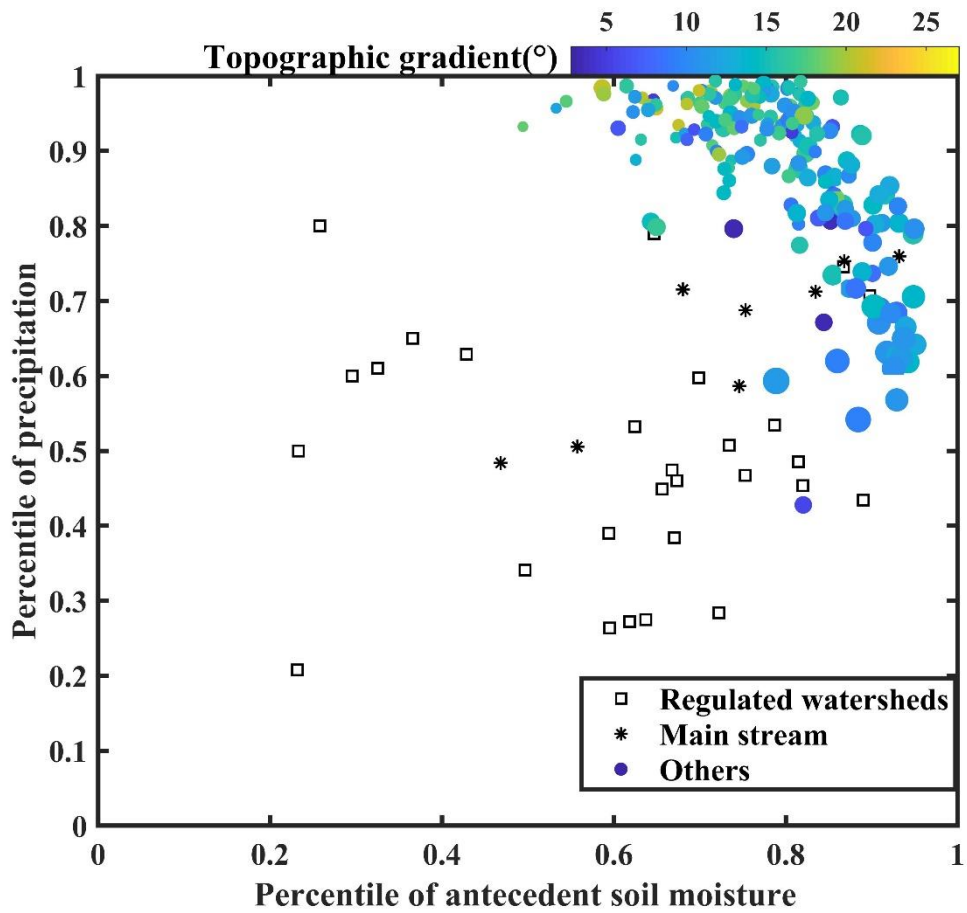
**Figure 5**: Scatterplot of the percentile of precipitation and antecedent soil moisture, the

851 color represents topographic gradient and the size of circles is scaled by drainage area.

852

853
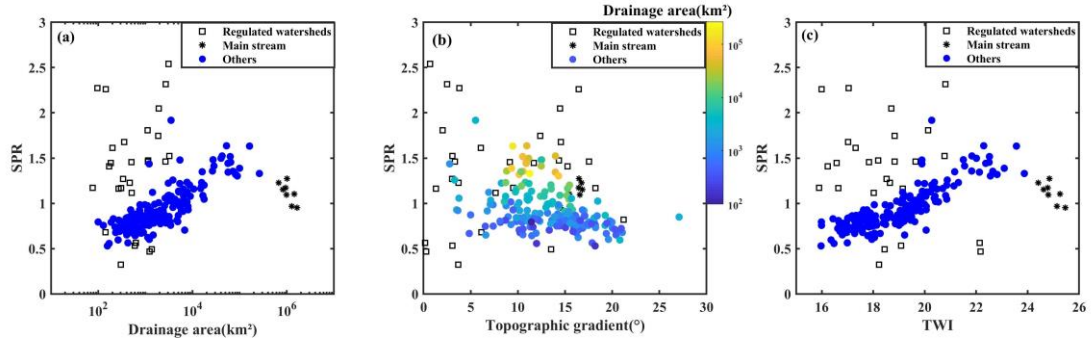
854

855 **Figure 6**: Scatterplots between the ratio of antecedent soil moisture and precipitation
856 (SPR) and (a) drainage area; (b) slope; and (c) topographic wetness index (TWI).
857

858
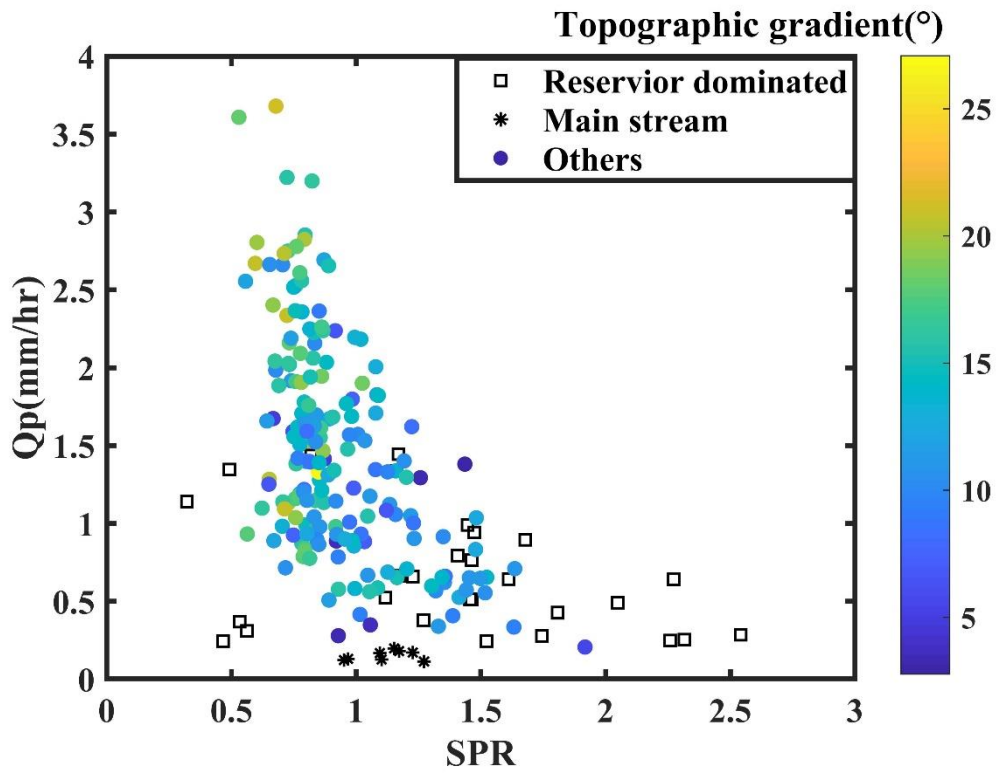
**Figure 7**: Scatterplot between the ratio of antecedent soil moisture and precipitation
(SPR) and area weighted annual maximum discharge ($Q_P$), the color represents
topographic gradient.

859
860
861
862

# Supplementary

Table S1: Estimated concentration time for 10 sites with largest drainage area: the ones on main stream (MS) and the ones at the outlets of major tributaries (TR).

| Site Name | Concentration Time (hr) | Drainage Area (km²) |
|-----------|-------------------------|---------------------|
| TR-Hukou | 17.9 | 161,979 |
| TR-Chenglingji | 18.8 | 261,986 |
| MS-Zhutuo | 32.7 | 668,661 |
| MS-Cuntan | 32.8 | 827,799 |
| MS-Wanxian | 37.6 | 948,524 |
| MS-Yichang | 41.5 | 982,948 |
| MS-Jianli | 45.2 | 1,014,690 |
| MS-Luoshan | 46.3 | 1,276,676 |
| MS-Hankou | 51.0 | 1,432,008 |
| MS-Datong | 54.3 | 1,657,604 |

872
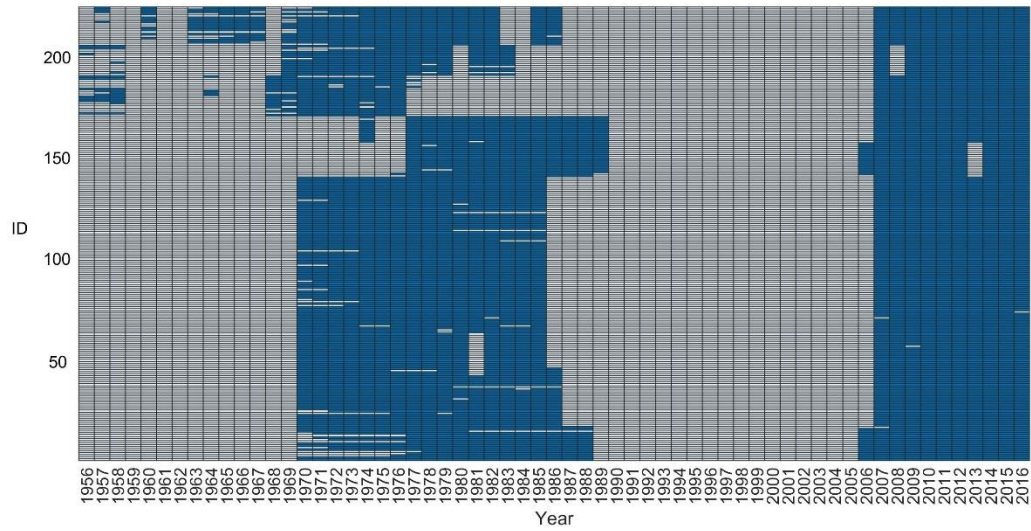
873 **Figure S1**: The data availability of each station, each column indicates each year while

874 each row is corresponding to each station, blue grid indicates there is record of this year.